

*Full Length Research paper*

# Impacts of whimsy and circular segment rotational speed on weld globule geometry in beat GMA welding of 5083 aluminum composite

**\*M. H. Ansari, Vishnu Mittal and E. A Singh**

Department of Mechanical Engineering, University of Calicut, Malappuram, India.

Accepted 21 January, 2015

The arc rotation mechanism system can be used to obtain the flat and broad weld bead due to the centrifugal force of the rotating arc at welding. In this investigation an arc rotation mechanism is developed and four input process parameters such as arc rotational speed, ratio of wire feed rate to travel speed, wire feed rate and eccentricity are considered. The experiments were conducted on square butt joint plate of 5083 H111 aluminum alloy using full factorial design of experiments. The mathematical models for penetration and convexity are developed using multiple nonlinear regression analysis and are checked for their adequacy. The confirmation experiments were conducted to verify the models. The mean analysis for penetration and convexity is done at all three levels of input process parameters. It is observed from the investigation that eccentricity has maximum effect on convexity followed by arc rotational speed, ratio of wire feed rate to travel speed and wire feed rate whereas wire feed rate have relative maximum effects on penetration.

**Key words:** Arc rotation mechanism, arc rotational speed, eccentricity, full factorial, square butt joint, aluminum alloy.

## INTRODUCTION

The quality of the weld joint depends on the weld bead shape and bead geometry such as bead width, height and penetration. The finger type penetration is predominant in pulsed GMAW which affects the quality of the welding. In arc rotation mechanism system, the arc is rotated continuously with certain speed during welding which results in flat and broad weld bead because of the centrifugal force of the rotating arc and penetration profile also can be improved. Some researchers have attempted arc rotation, arc oscillation and wire bending method for improving the weld bead characteristics. Sugitiani et al. (1991) developed automatic high speed rotating arc welding in which wire is mechanically rotated. Kang and Na (2003) studied the arc shape and bead characteristics in narrow groove gas metal arc welding by the use

electromagnetic arc oscillation, whereas Jeong et al. (2001) studied seam tracking controller of high speed rotating arc sensor developed by microprocessor using the variable space network method by modeling the heat flux from the molten end of the wire into the electrode. However, Rao (2004) developed the arc rotation mechanism and investigated the effect of arc rotational speed at constant eccentricity on weld bead geometry, but literatures are not available to study the effect of arc rotational speed at different eccentricity. So it is required to include the eccentricity as one of the factors for predicting the weld bead geometry. It is observed that very few literatures are available regarding the development of mathematical models to predict the weld bead geometry in arc rotation mechanism. Therefore it is necessary to develop the mathematical models to predict the weld bead geometry in arc rotation mechanism. Most of the researchers have attempted to estimate the input-output relationships by using statistical analysis and soft computing technique. In the statistical analysis, the

\*Corresponding author. E-mail: [ansari.mh@yahoo.co.in](mailto:ansari.mh@yahoo.co.in).

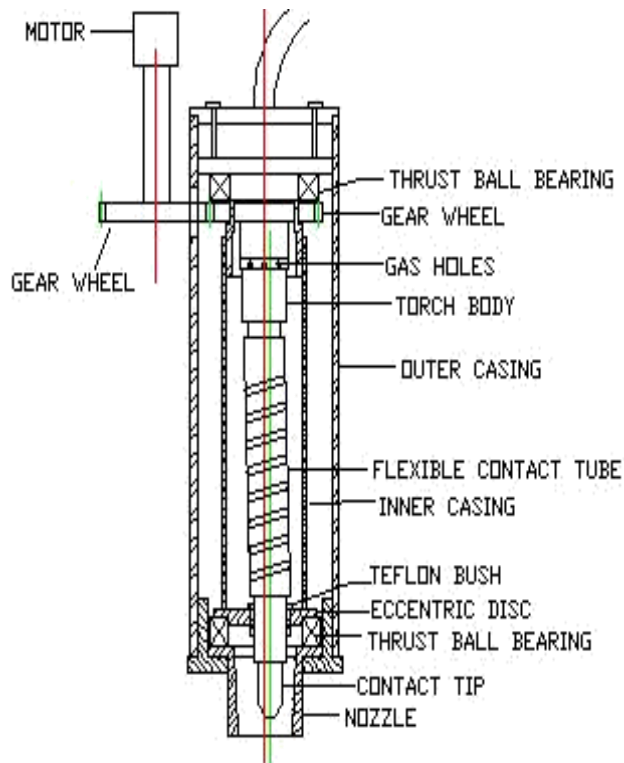


**Figure 1.** Arc rotation mechanism.

process parameters are expressed as linear as well as nonlinear functions and many researchers have formulated mathematical models to predict the weld bead geometry using different design of experiment techniques. In most of the cases, it is observed that nonlinear regression model can predict the weld bead geometry with greater accuracy than linear regression model. Rao et al. (2009) developed nonlinear regression model for prediction of bead geometry in pulsed GMA welding using Taguchi approach, while Kumar et al. (2009) developed mathematical models to predict the weld bead geometry using the second order polynomial equation. Conversely, Kim et al. (2003) investigated the sensitivity analysis and showed that the change of process parameters affects the bead width and height more strongly than penetration. Ganjigatti et al. (2008) established the relationships between the process parameters and responses for bead on plate type MIG welding process using regression analysis and the data was collected as per full-factorial design of experiments. Both linear as well as nonlinear regression analyses were employed to establish the input-output relations. Palani and Murugan (2006) studied the direct and interaction effects of process parameters on weld bead geometry. Siva et al. (2009) developed mathematical equations using multiple regression analysis, correlating various process parameters to weld bead geometry and the experiments were conducted based on a five factor, five level central composite rotatable design matrix. Kannan

and Yoganandh (2010) studied the effects of process parameters on clad bead geometry and its shape relationships. These results showed that the mathematical models developed by the statistical analysis from the experimental results can be used to predict the weld bead geometry. It is observed that most of the researchers have made study on bead on plate technique to develop the regression model which is not the actual welding environment and no literature is available in case of square butt joint welding. Therefore it is necessary to develop the regression model to predict the weld bead geometry on square butt joint plate. In the soft computing technique, neural network, fuzzy logic, neuro-fuzzy approach, genetic algorithm etc. are widely used to find the relationship between input and output parameters. Kim et al. (2002) developed an intelligent algorithm to predict process parameters on bead height through a neural network and multiple regression methods for robotic multi-pass welding process. Kanti and Rao (2008) Predicted weld bead geometry in pulsed GMA welding using back propagation neural network. Lee et al. (2006) developed an automatic SMAW control system based on an adaptive fuzzy sliding mode controller and mathematical model of the automatic welding control system formulated by analyzing the physical laws. Carrino et al. (2007) modeled a fuzzy logic based system to increase productivity in gas metal arc welding by optimising the deposition rate of the filler metal. Nagesh and Datta (2008) studied an integrated approach based on design of experiment, neural network and genetic algorithm for modeling using fractional factorial design of experiment technique. Moreover, Zhang et al. (2008) predicted weld profiles based on neural network analysis. In the present study, an attempt is made to develop the mathematical equations in arc rotation mechanism for predicting weld bead geometry which correlates the input process parameters like arc rotational speed, ratio of wire feed rate to travel speed (F/S), wire feed rate and eccentricity to convexity and penetration using full factorial design of experiment technique on square butt joint plate. The ratio of wire feed rate to travel speed is considered as a factor instead of travel speed to provide the proper travel speed for all combinations of wire feed rate. The main objectives of this study are to (1) develop the arc rotation mechanism system (2) develop the regression models for prediction of penetration and convexity (3) study the effect of process parameters on the bead geometry

## EXPERIMENTAL PROCEDURES

### Experimental details

Figures 1 and 2 represent a schematic diagram of the arc rotation mechanism system and a photograph of the corresponding experimental setup respectively.

As shown in Figure 1, the arc rotation mechanism consists of a flexible contact tube, eccentric disc, outer casing, inner casing,



Figure 2. Experimental setup.

sleeve, insulating bush, thrust ball bearing, nozzle, gear and dc motor. The flexible contact tube is made of copper tube which is cut in helical shape with helix angle  $30^\circ$  to give it flexibility to move in lateral direction so that the arc can be rotated. It also provides path for current flow between the torch and rotating contact tip. The design should provide long working life as well as flexibility for movement with little force. The thickness, outer diameter and length of the contact tube are 1.5, 14 and 100, respectively. These dimensions provide necessary flexibility and the flexible contact tube conducts high current without overheating. Two sleeves of copper material are brazed at both ends of the contact tube so that it can be fitted between the torch body and contact tip by threading. Three different eccentric discs are made to rotate the arc with different eccentricity and only one eccentric disc is used at a time. The adpoter for gear mounting is brazed to one end of the inner casing and other end of it is externally threaded to fit the required eccentric disc which is internally threaded. Two thrust bearings are placed at both end of the inner casing. Insulating bush made of teflon material is used as insulating material between the eccentric disc hole and sleeve so that current does not pass from flexible tube and sleeve to the other parts of the system. During welding the inner casing is mechanically rotated by a set of gears using 500 W DC motor at different speeds controlled by rheostat which gives the lateral movement to the flexible tube and finally the contact tip rotates and hence arc rotates during welding. The rotational speed is measured by noncontact type tachometer. The marine grade non-heat treatable high strength aluminum alloy 5083 H111 plate of 6.35 mm thickness is used as base material. This material possess excellent corrosion resistance, excellent weldability and reduced sensitivity to hot cracking when welded with Al-Mg alloyed filler wire and finds application in ship building industry, structural and pressure vessel industries (Mutombo and Toit, 2010). The plate is cut into the required size of 160 × 100 mm by using circular saw machine. Shaper machine is used for machining square butt joint of the plate. The melting point of the oxide layer is nearly three times more than aluminum therefore before conducting the experiments the top surface of the test plates are cleaned by means of acetone and then stainless steel wire brush is used to remove the oxide layer from the welding area of the base material (Mathers, 2002).

The experiments are conducted by laying a single bead on square butt joint plate with zero gap between both plates using aluminum alloy 5183 welding wire of 1.2 mm diameter. The chemical compositions of base metal and welding wire material are given in Table 1.

Experiments are carried out using Kemppi Pro Evolution 3200 welding machine and the weld beads are deposited using pulsed GMA welding. Pure argon gas is used as shielding material and is supplied at the rate of 17 l/min. Direct current electrode positive (DCEP) with electrode to work angle and the distance between the contact tip and work piece is maintained at  $90^\circ$  and 17 mm respectively. The work is fixed on a platform whose speed is controlled by rheostat and moves below the torch.

### Conducting the experiments

The four input process parameters considered for conducting the experiments were identified. They are arc rotational speed (N), ratio of wire feed rate to travel speed (F/S), wire feed rate (F) and eccentricity (E). A large number of trial experiments are conducted with the square butt joint plate by varying one of the process parameters while keeping remaining parameters at constant value, to find the proper range of the process parameters. The absence of visible defects and smooth bead appearance are considered for deciding the range. The selected values of the process parameters together with their units and notations are given in Table 2. The experiments are conducted using full factorial design of experiment (Montgomery, 2006). As per this technique, total numbers of experiments considered for conducting the experiments are  $3^4=81$  as there are four input process parameters each at three levels. The levels for input process parameters were considered based on the preliminary studies conducted.

### Measuring the dimensions of bead geometry

The weld bead samples are marked at three positions with the first mark being positioned at middle of the weld bead and the other two at a distance of 30 mm on both sides of the mid mark for each sample. These marked positions are cut by using circular saw machine to get the metallographic weld bead samples. The emery paper of grade 120, 220,320, 420, 4/0 and 5/0 in order are used for grinding the transverse face of the weld bead sample and then the specimens are polished by using aluminum oxide powder and velvet cloth in a polishing machine. The polished specimens are cleaned with ethyl alcohol and caustic etchant (15 g NaOH+100 g distilled water) solution is applied to reveal the bead geometry of the macro-etched samples. Then the parameters, such as bead height (H), bead width (W) and bead penetration (P) as shown in Figure 3 are measured using AutoCAD software. In measuring these parameters, first the photograph of each macro-etched sample is scanned by using a scanner (model s2w 3300U) at 1600 dpi resolutions and then imported to AutoCAD software. As the picture dimensions are different from the real dimensions of the weld bead, there is need to calculate the scale factor. As such, in calculating it, the plate thickness is measured on the pictures using AutoCAD. By knowing the actual plate thickness (6.35mm) and the plate thickness on the picture, the scale factor is calculated, and then the bead geometry dimensions are measured on the picture, while the actual dimensions of the weld bead are calculated by using the scale factor.

Further, the dimensions of the weld bead are measured using a toolmakers microscope to check the accuracy of the measurement. The averages of these three readings for each weld bead samples are given in Table 3. The convexity (C) of the weld bead is also mentioned in the same Table 3 which is the ratio of bead height (H) and bead width (W).

**Table 1.** Chemical composition of materials used.

S/N	Materials used	Element weight %							
		Si	Fe	Cu	Mn	Mg	Cr	Zn	Ti
1	5083 H111	0.1	0.16	0.02	0.5	4.6	0.07	0.03	0.06
2	5183	0.17	0.24	0.05	0.78	4.95	0.08	-	0.02

**Table 2.** Input parameters and their limits.

Input parameter	Units	Notation	Factor levels		
			-1	0	1
Rotational speed	rpm	N	100	500	900
Wire feed rate / travel speed (F/S)	—	X	30	40	50
Wire feed rate	m/min	F	4	5.5	7
Eccentricity	mm	E	2.0	3.5	5.0

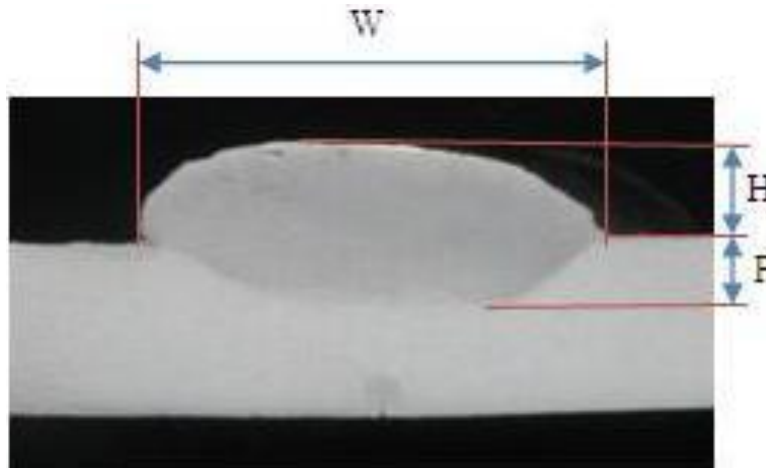


**Figure 3.** Transverse section of weld bead after macro-etching of experimental run 40. W: bead width, H: bead height, P: bead Penetration.

**Mathematical models**

The experimental results as given in Table 3 are employed to find the mathematical relationship between input process parameters and bead geometry. The relationship between output parameters (penetration or convexity) and input process parameters (arc rotational speed, ratio of wire feed rate to travel speed, wire feed rate and eccentricity) for multiple nonlinear regression analysis can be expressed as:

$$Y = aN^bX^cF^dE^e$$

where Y is penetration or convexity; N — arc rotational speed (rpm); X — wire feed rate / travel speed; F — wire feed rate (m/min) E — eccentricity (mm); a, b, c, d, and e — regression coefficients

The values of the regression coefficients of the above model are calculated by using OriginPro8.1 software (Origin, 2010). The mathematical models developed by this software are presented below:

$$P = \frac{0.0231X^{0.6393}F^{2.5005}}{N^{0.2219}E^{0.9698}} \tag{1}$$

$$C = \frac{0.7168X^{0.2030}}{N^{0.1087}F^{0.1797}E^{0.7935}} \tag{2}$$

**Checking the accuracy of the model**

The mathematical models developed above are checked for their accuracy using ANOVA technique, plotting a scattered graph and conducting the confirmation experiments.

**ANOVA**

The mathematical models developed for penetration and convexity

**Table 3.** Dimensions of weld bead geometry.

Bead No.	Bead geometry and Convexity			
	P(mm)	H(mm)	W(mm)	C
B 01	1.01	4.24	10.05	0.4219
B 02	0.73	3.75	11.5	0.3261
B 03	0.67	3.5	12.34	0.2836
B 04	1.21	4.75	11.18	0.4249
B 05	0.85	4.53	13.11	0.3455
B 06	0.75	4.15	13.91	0.2983
B 07	1.51	5.51	12.75	0.4322
B 08	1.01	4.92	14.03	0.3507
B 09	0.85	4.81	14.93	0.3222
B 10	2.91	4.05	10.52	0.385
B 11	2.22	3.95	11.69	0.3379
B 12	1.41	3.84	12.81	0.2998
B 13	3.16	4.85	12.02	0.4035
B 14	2.5	4.8	13.73	0.3496
B 15	1.88	4.54	15.06	0.3015
B 16	3.93	5.63	13.41	0.4198
B 17	2.78	5.38	15.04	0.3577
B 18	2.35	5.2	15.59	0.3335
B 19	5.35	4.1	13.21	0.3104
B 20	3.89	4.02	13.06	0.3078
B 21	2.83	3.91	13.93	0.2807
B 22	5.62	4.8	14.3	0.3357
B 23	4.07	4.82	15.08	0.3196
B 24	3.23	4.8	15.57	0.3083
B 25	6.35	5.4	15.9	0.3396
B 26	4.56	5.21	16.21	0.3214
B 27	4.23	5.3	17.04	0.311
B 28	0.6	3.17	12.64	0.2508
B 29	0.46	3.01	13.31	0.2261
B 30	0.35	2.72	14.86	0.183
B 31	0.73	3.91	14.7	0.266
B 32	0.58	3.68	15.86	0.232
B 33	0.47	3.41	17.5	0.1949
B 34	0.83	4.36	15.72	0.2774
B 35	0.71	4.01	16.37	0.245
B 36	0.63	3.72	18.02	0.2064
B 37	1.56	3.15	13.58	0.232
B 38	1.21	2.99	15.02	0.1991
B 39	0.92	2.79	15.85	0.176
B 40	1.97	3.95	14.98	0.2637
B 41	1.41	3.78	17.01	0.2222
B 42	1.03	3.54	18	0.1967
B 43	2.38	4.5	16.95	0.2655
B 44	1.8	4.4	17.09	0.2575
B 45	1.54	4.07	19.55	0.2082
B 46	2.58	3.31	14.42	0.2295
B 47	1.96	3.08	15.17	0.203
B 48	1.5	2.86	17.16	0.1667
B 49	3.29	4.02	17.15	0.2344
B 50	2.28	3.9	17.2	0.2267
B 51	1.95	3.63	19.66	0.1846
B 52	4.01	4.65	18.2	0.2555
B 53	3.3	4.53	18.84	0.2404
B 54	2.43	3.97	21.08	0.1883
B 55	0.51	2.53	14.21	0.178
B 56	0.4	2.35	15.42	0.1524
B 57	0.31	2.21	16.51	0.1339
B 58	0.58	3.11	16.45	0.1891
B 59	0.45	2.98	17.73	0.1681

**Table 3.** Contd.

B 60	0.39	2.76	18.95	0.1456
B 61	0.63	3.53	17.29	0.2042
B 62	0.51	3.5	18.75	0.1867
B 63	0.41	3.03	20	0.1515
B 64	1.14	2.62	15.42	0.1699
B 65	0.7	2.45	16.8	0.1458
B 66	0.51	2.25	18.03	0.1248
B 67	1.23	3.33	17.73	0.1878
B 68	0.82	3.08	19.38	0.1589
B 69	0.7	2.72	20.75	0.1311
B 70	1.49	3.75	18.75	0.2
B 71	1.25	3.45	20.12	0.1715
B 72	0.93	3.12	22.07	0.1414
B 73	1.65	2.65	16.54	0.1602
B 74	1.2	2.5	17.75	0.1408
B 75	1.1	2.32	19.31	0.1201
B 76	2.3	3.43	18.25	0.1879
B 77	1.57	3.4	19.05	0.1785
B 78	1.4	2.93	22.01	0.1331
B 79	3.06	3.92	19.57	0.2003
B 80	2.3	3.62	20.08	0.1803
B 81	1.43	3.21	23.71	0.1354

**Table 4.** Analysis of variance for mathematical model.

Model	Standard error of estimate	Coefficient of determination (R <sup>2</sup> )	Adjusted R <sup>2</sup> (%)
Penetration	0.1952	0.9798	97.87
Convexity	0.0163	0.9627	96.07

as given in equations (1) and (2) respectively are tested using analysis of variance (ANOVA) technique which is presented in Table 4 .These values indicate that the regression model is quite accurate.

**Scatter graphs**

The scatter graphs of penetration and convexity model are shown in Figures 4 and 5, respectively which plots the graph between observed values by the experiment and predicted values by the mathematical model.

The observed values and predicted values of these responses (convexity and penetration) are scattered close to the 45° line, indicating good fit of the developed mathematical models so the model is quite accurate. It is also observed that the percentage error is less than 15% in all the cases except one in the case of convexity, and less than 23% except one in the case of penetration. Hence, it is concluded that the model can be used to predict the convexity and penetration in arc rotation mechanism with good accuracy.

**Confirmation experiments**

Further, to validate the above developed models, two more experiments were conducted using different values of input process parameters other than those used in the design matrix:

$$\%Error = \frac{(\text{Measured Value}-\text{Predicted Value})}{\text{Predicted Value}} \times 100$$

The dimensions of the bead geometry are measured using the same procedure as described in above (Measuring the dimensions of bead geometry section). The details of the confirmation experiments are given in Table 5 and it shows that the result is quite satisfactory.

**RESULTS AND DISCUSSION**

**Analysis of results for penetration**

As given in Table 3 it is observed that the penetration varies from 0.31 to 6.35 mm. The mean analysis for penetration is given in Table 6 which provides the data for the average effect of each factor at different levels. These values are calculated by taking the average of penetration value for that factor at that particular level from Table 3. is the difference between the maximum and minimum values of mean penetration within that factor. The effect of each factor is positioned as per the magnitude of values. The first position factor has the

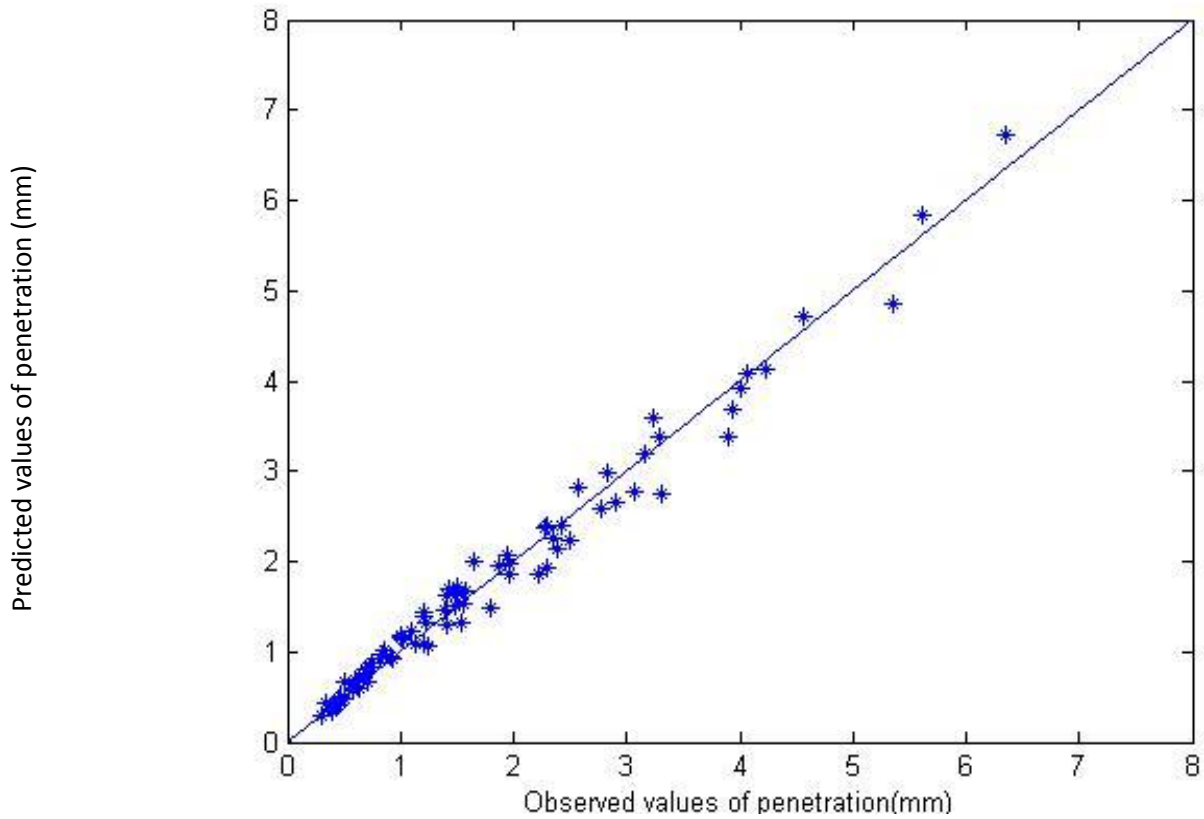


Figure 4. Scatter graph for penetration model.

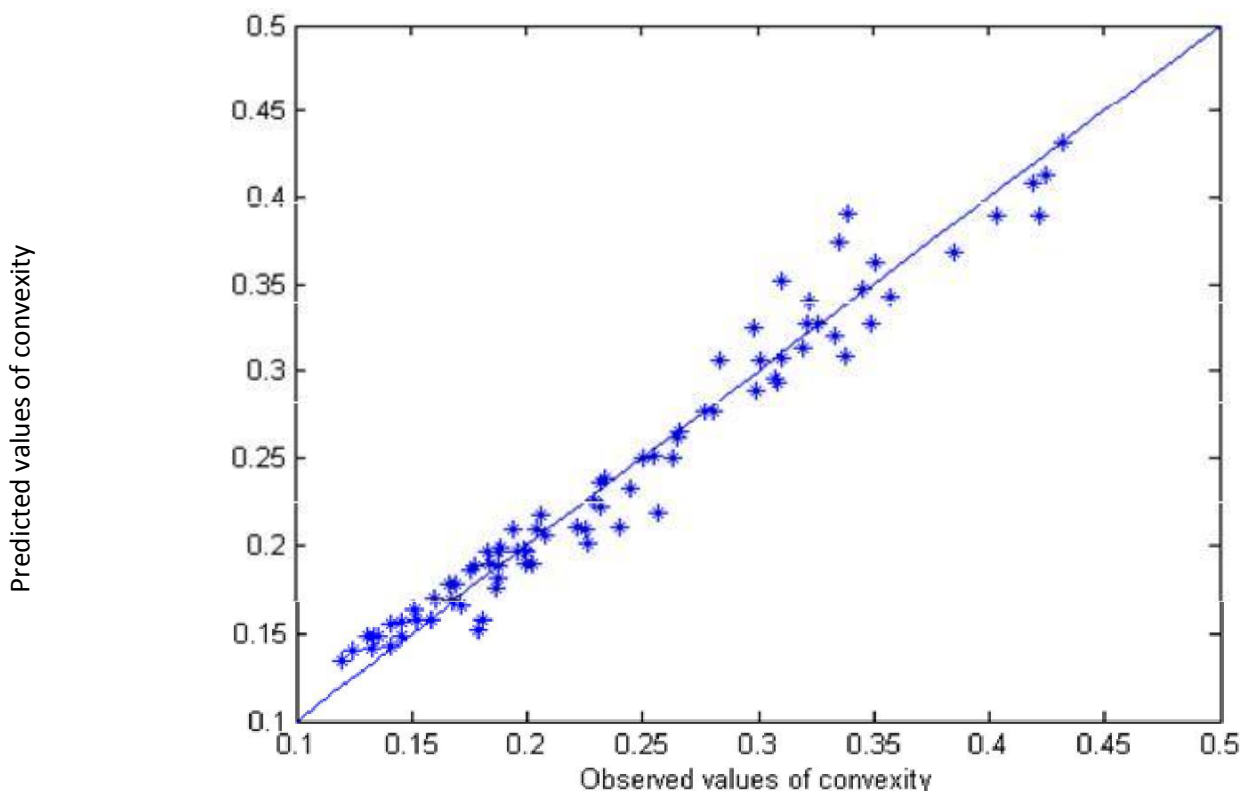


Figure 5. Scatter graph for convexity model.

**Table 5.** Results of confirmation experiment.

Expt. No.	Input parameters				Measured values				Predicted values		% error	
	N	X	F	E	P	W	H	C	P	C	P	C
CE1	300	35	5	3.5	1.13	15.65	3.15	0.2013	1.03	0.2179	9.71	-7.62
CE2	700	45	5	5	0.67	19.43	3.36	0.1729	0.72	0.1591	-6.94	8.67

**Table 6.** Mean analysis for penetration.

	N	X	F	E
Level1	2.281	1.469	0.672	2.661
Level2	1.686	1.719	1.694	1.573
Level3	1.340	2.119	2.942	1.073
	0.941	0.650	2.270	1.588
Position	3	4	1	2
SD	1.339			

**Table 7.** Mean analysis for convexity.

	N	X	F	E
Level1	0.2750	0.2276	0.2517	0.3418
Level2	0.2426	0.2440	0.2459	0.2234
Level3	0.2096	0.2557	0.2296	0.1621
	0.0654	0.0281	0.0221	0.1797
Position	2	3	4	1
SD	0.082			

maximum effect and fourth position factor has minimum effect on penetration. The following observations can be drawn from Table 6:

- (i) Among all the four input parameters, the wire feed rate has maximum effect on penetration. By increasing the wire feed rate from 4 to 7 m/min, the mean penetration is increased by 2.270 mm.
- (ii) Eccentricity has the next effect on penetration. By increasing the eccentricity from 2 to 5 mm, the mean penetration is decreased by 1.588 mm.
- (iii) By increasing the arc rotational speed from 100 to 900 rpm, the mean penetration is reduced by 0.941 mm.
- (iv) The ratio of wire feed rate to travel speed has least effect on penetration and by increasing its value from 30 to 50; the penetration is increased by 0.650 mm.

**Analysis of results for convexity**

It is observed from Table 3 that the convexity index varies from 0.1201 to 0.4322. The mean analysis for convexity is given in Table 7. The following observations can be drawn from Table 7:

- (i) Among all the four input parameters, eccentricity has maximum effect on convexity. By increasing the eccentricity from 2 to 5 mm, the mean convexity is reduced by 0.1797.
- (ii) Arc rotational speed has the next effect on convexity. By increasing the rotational speed from 100 to 900 rpm, the mean convexity is reduced by 0.0654.
- (iii) By increasing the ratio of wire feed rate to travel speed from 30 to 50, the mean convexity is increased by 0.0281.
- (iv) Wire feed rate has minimum effect on convexity. By increasing the wire feed rate from 4 to 7 m/min, the mean convexity is decreased by 0.0221.

**Conclusions**

The following conclusions can be obtained from this study:

- (i) Eccentricity has maximum effect on convexity followed by arc rotational speed, ratio of wire feed rate to travel speed and wire feed rate.
- (ii) Wire feed rate has maximum effect on penetration

followed by eccentricity, arc rotational speed and ratio of wire feed rate to travel speed.

(iii) With an increase in the value of eccentricity and rotational speed, bead height decreases and width increases because of the flat and broad weld bead produced by the rotating arc.

(iv) The mean convexity and the mean penetration ranges from 0.1621 to 0.3418 and 0.672 to 2.942 mm, respectively.

(v) The coefficient of determination of penetration and convexity model is 0.9798 and 0.9627, respectively which indicates that the model can predict these weld bead geometry with good accuracy.

## REFERENCES

- Carrino L, Natale U, Nele L, Sabatini ML, Sorrentino L (2007). A neuro-fuzzy approach for increasing productivity in gas metal arc welding processes. *Int. J. Adv. Manuf. Technol.*, 32: 459-467.
- Ganjigatti JP, Pratihari DK, Choudhury AR (2008). Modeling of the MIG welding process using statistical approaches. *Int. J. Adv. Manuf. Technol.*, 35: 1166-1190.
- Jeong S, Lee GY, Lee WK, Kim SB (2001). Development of high speed rotating arc sensor and seam tracking controller for welding robots, *IEEE, ISIE*, Korea, pp. 845-850.
- Kang YH, Na SJ (2003). Characteristics of welding and arc signal in narrow groove gas metal arc welding using electromagnetic arc oscillation, *Supplement to the welding journal*, sponsored by the American welding society and the welding research council, pp. 93-99-s.
- Kannan T, Yoganandh J (2010). Effect of process parameters on clad bead geometry and its shape relationships of stainless steel claddings deposited by GMAW. *Int. J. Adv. Manuf. Technol.*, 47: 1083-1095.
- Kanti KM, Rao PS (2008). Prediction of bead geometry in pulsed GMA welding using back propagation neural network. *J. Mater. Process Technol.*, 200: 300-305.
- Kim IS, Son JS, Park CE, Lee CW, Prasad YKDV (2002). A study on prediction of bead height in robotic arc welding using a neural network. *J. Mater. Process Technol.*, 130-131: 229-234.
- Kim IS, Son KJ, Yang YS, Prasad YKDV (2003). Sensitivity analysis for process parameters in GMA welding processes using a factorial design method. *Int. J. Mach. Tools Manuf.*, 43:763-769.
- Lee CY, Pi-Cheng T, Wen-Hou C (2006). Adaptive fuzzy sliding mode control for an automatic arc welding system. *Int. J. Adv. Manuf. Technol.*, 29: 481-489.
- Mathers G (2002). *The welding of aluminium and its alloys*, Woodhead Publishing Limited, Cambridge, England, 4: 66.
- Montgomery DC (2006). *Design and analysis of experiments*, 5<sup>th</sup> edn. Wiley, New York, pp. 367-372.
- Mutombo K, Toit MD (2010). Mechanical properties of 5083 aluminium welds after manual and automatic pulsed gas metal arc welding using E5356 filler. *Mater. Sci. Forum*, 654-656: 2560-2563, doi10.4028/www.scientific.net/MSF.654-656.2560.
- Nagesh DS, Datta GL (2008). Modeling of fillet welded joint of GMAW process: integrated approach using DOE, ANN and GA. *Int. J. Interact. Des. Manuf.*, 2: 127-136.
- OriginPro8.1 (2010). OriginLab Corporation.
- Palani PK, Murugan N (2006). Development of mathematical models for prediction of weld bead geometry in cladding by flux cored arc welding. *Int. J. Adv. Manuf. Technol.*, 30: 669-676.
- Rao PS (2004). Development of arc rotation mechanism and experimental studies on pulsed GMA welding with and without arc rotation, Ph.D. thesis, IIT Kharagpur.
- Rao PS, Gupta OP, Murty SSN, Rao ABK (2009). Effect of process parameters and mathematical model for the prediction of bead geometry in pulsed GMA welding. *Int. J. Adv. Manuf. Technol.*, 45: 496-505.
- Siva K, Murugan N, Logesh R (2009). Optimization of weld bead geometry in plasma transferred arc hardfaced austenitic stainless steel plates using genetic algorithm. *Int. J. Adv. Manuf. Technol.*, 41: 24-30.
- Sugitani Y, Kobayashi Y, Murayama M (1991). Development and application of automatic high speed rotation arc welding. *Welding int.*, 5(7):577-583.
- Zhang X, Daneryd A, Holmgren B, Skarin D (2008). Arc and weld profile predictions for zinc-coated thin steel plates, proceedings of the 8<sup>th</sup> international conference on Trends in welding research, Georgia, USA, pp. 339-347.

**APPENDIX**

**Appendix 1.** Design matrix as per full factorial design.

	Parameters and their levels			
	N	X	F	E
1	-1	-1	-1	-1
2	0	-1	-1	-1
3	1	-1	-1	-1
4	-1	0	-1	-1
5	0	0	-1	-1
6	1	0	-1	-1
7	-1	1	-1	-1
8	0	1	-1	-1
9	1	1	-1	-1
10	-1	-1	0	-1
11	0	-1	0	-1
12	1	-1	0	-1
13	-1	0	0	-1
14	0	0	0	-1
15	1	0	0	-1
16	-1	1	0	-1
17	0	1	0	-1
18	1	1	0	-1
19	-1	-1	1	-1
20	0	-1	1	-1
21	1	-1	1	-1
22	-1	0	1	-1
23	0	0	1	-1
24	1	0	1	-1
25	-1	1	1	-1
26	0	1	1	-1
27	1	1	1	-1
28	-1	-1	-1	0
29	0	-1	-1	0
30	1	-1	-1	0
31	-1	0	-1	0
32	0	0	-1	0
33	1	0	-1	0
34	-1	1	-1	0
35	0	1	-1	0
36	1	1	-1	0
37	-1	-1	0	0
38	0	-1	0	0
39	1	-1	0	0
40	-1	0	0	0
41	0	0	0	0
42	1	0	0	0
43	-1	1	0	0
44	0	1	0	0

## Appendix 1. Contd.

---

45	1	1	0	0
46	-1	-1	1	0
47	0	-1	1	0
48	1	-1	1	0
49	-1	0	1	0
50	0	0	1	0
51	1	0	1	0
52	-1	1	1	0
53	0	1	1	0
54	1	1	1	0
55	-1	-1	-1	1
56	0	-1	-1	1
57	1	-1	-1	1
58	-1	0	-1	1
59	0	0	-1	1
60	1	0	-1	1
61	-1	1	-1	1
62	0	1	-1	1
63	1	1	-1	1
64	-1	-1	0	1
65	0	-1	0	1
66	1	-1	0	1
67	-1	0	0	1
68	0	0	0	1
69	1	0	0	1
70	-1	1	0	1
71	0	1	0	1
72	1	1	0	1
73	-1	-1	1	1
74	0	-1	1	1
75	1	-1	1	1
76	-1	0	1	1
77	0	0	1	1
78	1	0	1	1
79	-1	1	1	1
80	0	1	1	1
81	1	1	1	1

---